INSTITUTE OF PHYSICS PUBLISHING JOURNAL OF PHYSICS: CONDENSED MATTER

J. Phys.: Condens. Matter **13** (2001) 6285–6295 PII: S0953-8984(01)23882-X

Point contact characteristics of $NbSe_3$ in the superconducting state

R Escudero[1], **A Briggs**[2] **and P Monceau**[2]

[1] Instituto de Investigaciones en Materiales, Universidad Nacional, Autónoma de México, Apartado Postal 70-360 México, Distrito Federal, 04510 México
[2] Centre de Recherches sur les Trés Basses Températures, CNRS, BP 166X, 38042 Grenoble Cedex, France

Received 11 April 2001, in final form 11 April 2001
Published 6 July 2001
Online at stacks.iop.org/JPhysCM/13/6285

Abstract

A study of the electronic properties of $NbSe_3$ using $NbSe_3$–$NbSe_3$ junctions has been made. Structures in the current against voltage curves and in the differential resistance against voltage curves were observed and studied as functions of temperature between 8 K and 0.4 K and magnetic field up to 1 T. Analysis of the data shows that the pressure applied at the contact is sufficient to make $NbSe_3$ superconducting.

1. Introduction

The study of the electronic properties of systems of restricted dimensionality is of interest because they frequently show one or more collective properties [1]. At low temperatures charge density waves (CDWs), spin density waves (SDWs), superconductivity and magnetism may appear, depending on the predominant electronic interaction in the system. CDWs and SDWs occur through nesting of the Fermi surface. In many systems only some portions of the Fermi surface are nested and the electrons (holes) taking part in the nesting process are those that are directly responsible for the formation of an energy gap in the SDW or CDW condensates. If the electronic interaction is mediated by phonons, then in general there will be competition between the formation of a CDW ground state and one of superconducting character. Both kinds of phenomena are self-excluding, because in general they compete for the same portions of the Fermi surface. In this context $NbSe_3$ is an interesting compound because it shows both phenomena, i.e. competition between CDWs and superconductivity.

$NbSe_3$ is a low-dimensional metallic compound, which presents two CDW transitions occurring at temperatures of about $T_1 = 145$ K and $T_2 = 59$ K, due to the nesting of different parts the Fermi surface. These transitions can be seen as two anomalies in the resistivity against temperature characteristic (ρ–T) which shows a sharp increase of $\rho(T)$ just below the transition temperatures. The nesting of different portions of the Fermi surface opens energy gaps because of the formation of two incommensurable CDWs. Experimental studies have

shown that the two CDWs are essentially independent and non-interacting, and can be ascribed to two different chains of the crystalline structure of the material [2]. The formation of the CDW uses a certain number of electrons to form the new ground state. The process destroys fractions of the Fermi surface in the nesting direction, which is the reason for the observed drop of the conductivity. Ong and Monceau [3] calculated the fraction of the Fermi surface destroyed at the two transitions. At 145 K the fraction is only about 20%, whilst at 59 K it is about 62% of the remaining 80% of the Fermi surface. Consequently, $NbSe_3$ remains metallic at lower temperatures, as can be observed in the $\rho(T)$ curves.

The nesting on the Fermi surface has the obvious consequence of diminishing the total electronic population available for transport properties. Due to this low remaining electronic density, the superconducting transition is then precluded. However, experiments performed under pressure show that superconductivity develops with moderate external pressures, and that the superconducting transition is strongly dependent on the pressure. Previous studies applying moderate pressures have shown that, at first, the CDW anomaly in the $\rho(T)$ at T_2 decreases, while the superconducting transition T_c increases, until a critical pressure of about 0.6 GPa [4]. A superconducting transition temperature of about $T_c = 2.5$ K is obtained, when the CDW at T_2 is completely destroyed. With further increase of the external pressure T_c decreases. Nuñez-Regueiro *et al* [2] found that T_1 continuously decreases under pressure, and it is completely destroyed above 3.6 GPa. The superconducting transition temperature begins to increase again when the T_1 CDW starts to disappear. The maximum superconducting temperature at the critical pressure of 3.6 GPa measured by Nuñez-Regueiro *et al* was about $T_c \simeq 5$ K. Then with further increase in pressure the critical temperature decreases. An important observation made by these workers, was that when the T_2 CDW is destroyed, and superconductivity develops, both phenomena occur on the same crystallographic chains. This behaviour was also found for the superconducting state which is sustained by destroying the other crystallographic chains related to the T_1 transition.

Finally, an interesting point concerning superconductivity and CDW condensates is that the nature of the processes involved are similar. Thus, many of the phenomena that occur for the creation of a CDW state appear also in superconductivity. The physical mechanisms used to explain both phenomena are similar in a sense, for instance the evolution with temperature of the energy gap is expected to be similar for both systems. In this paper we describe our results for point contact junctions, made using a novel technique, between $NbSe_3$–$NbSe_3$, at low temperatures; and their use to investigate the superconducting state in $NbSe_3$.

2. Experiment

A simple method of forming a tunnel junction or point contact is to put a wire counter-electrode in contact with the specimen. If either the wire or specimen is oxidized or dirty, a junction is formed. This technique was used in studies of Escudero *et al* [5], but little attention has been paid to the possible effect of the local pressure in the junction. To obtain reliable junctions the counter-electrode must exert some pressure, and depending on the contact area and the tension on the counter-electrode considerable pressures (gigapascals) may be exerted on the specimen at the junction, and may modify material properties in its vicinity. The junctions fabricated for the present experiments consisted of two $NbSe_3$ ribbons crossed perpendicularly, one on the other. The junctions were formed on a cylindrical glass rod of about 100 μm diameter, used as support for the ribbons. The ribbon of $NbSe_3$ lay along the glass cylinder, the counter-electrode was stretched perpendicularly across the $NbSe_3$, pressing on it to make electrical contact; this is illustrated in the inset of figure 1. High-purity $NbSe_3$ ribbons with resistance ratios $R_{300\ \mathrm{K}}/R_{4\ \mathrm{K}} \sim 200$ were used throughout. The ribbon widths were of the order of 5–30 μm.

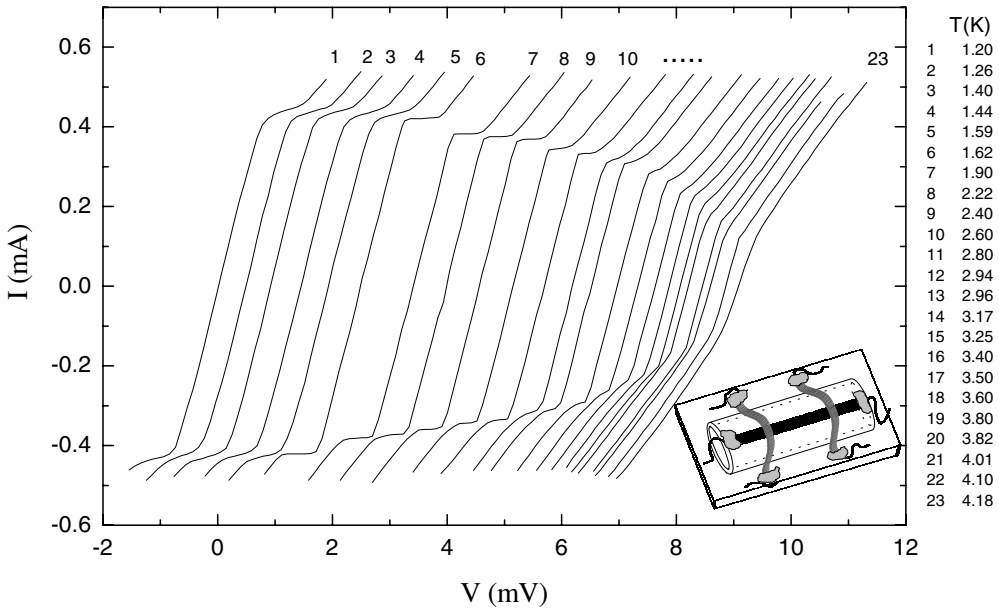

Figure 1. Current against voltage characteristics of a junction of $NbSe_3$–$NbSe_3$ at different temperatures, from 1.2 K to 4.179 K. The curves have been displaced horizontally for clarity.

High-purity $NbSe_3$ was used to avoid the existence of filamentary superconductivity which might occur if impurities were present. Various regimes may be distinguished for determining the spectroscopic characteristics of point contact tunnel junctions [6–9]. Two parameters are important: the resistance of the contact and the Knudsen number, K. The latter parameter depends on the electronic mean free path, l, and on the radius of the contact, a; K is given by the ratio $K = l/a$. In our point contacts the resistance varies from values $1\ \Omega \leqslant R \leqslant 20\ \Omega$. If we use the formula of Wexler [7], given by

$$R = \frac{4\rho l}{3\pi a^2} + \Gamma(K)\frac{\rho}{2a} \tag{1}$$

we obtain the fact that our point contacts are in the limit: $0.2 \leqslant K \leqslant 1$. Here we used the following values: $\Gamma(K) \simeq 0.77$, a mean free path of $l \sim 1000$ Å, and a resistivity of $NbSe_3$ at 4 K of $\rho_{4\,\mathrm{K}} \simeq 5\ \mu\Omega$ cm. Thus, our point contacts are close to the ballistic limit[3] and spectroscopic features can be extracted with little smearing. Figure 1 shows typical behaviour for a $NbSe_3$–$NbSe_3$ contact measured between 1.2 K and 4.2 K. The data is shown as full curves, the critical current I_c ($T = 1.2$ K) has the value of 420 μA, and the normal resistance is $R_N = 4.9\ \Omega$. Figure 2 shows the temperature evolution of the critical current I_c. The superconducting transition temperature deduced from figures 1 and 2 for this junction is about 4.18 K. The normal resistance of the junction was taken at a high voltage, and the resistance in the low-voltage region (less than 1 mV) is of the order of 1.667 Ω. Figure 3 shows the differential resistance $(\mathrm{d}V/\mathrm{d}I)_{V=0}$, measured at zero bias and its evolution with temperature. This figure shows the onset of superconductivity at around 4.18 K; the transition is completed at 3.5 K.

[3] The ballistic regime is defined as the limit when the electronic mean free path, l, is much larger than the radius of the constriction, a: $l \gg a$.

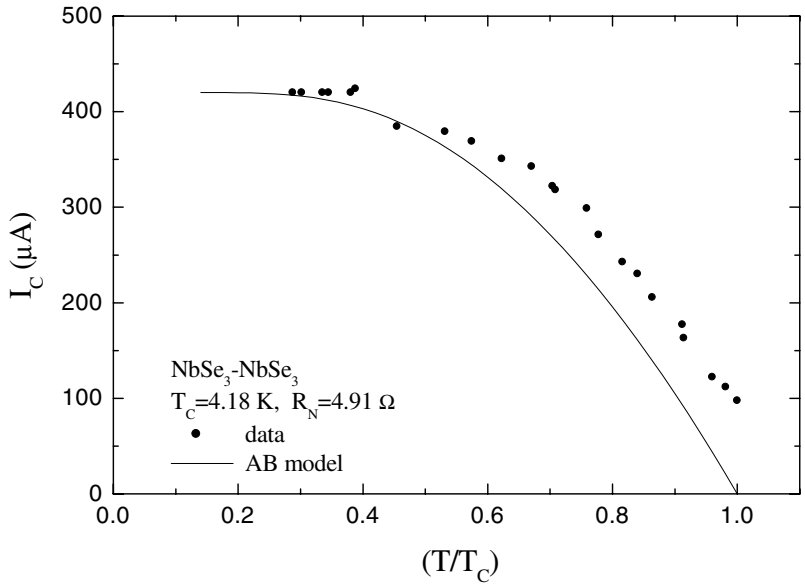

Figure 2. Critical current against the normalized temperature for a junction of $NbSe_3$–$NbSe_3$, full circles. The transition temperature was $T_c = 4.18$ K, $R_N = 4.91$ Ω and the critical current extrapolated to zero temperature was 420 μA. The full curve is the AB model.

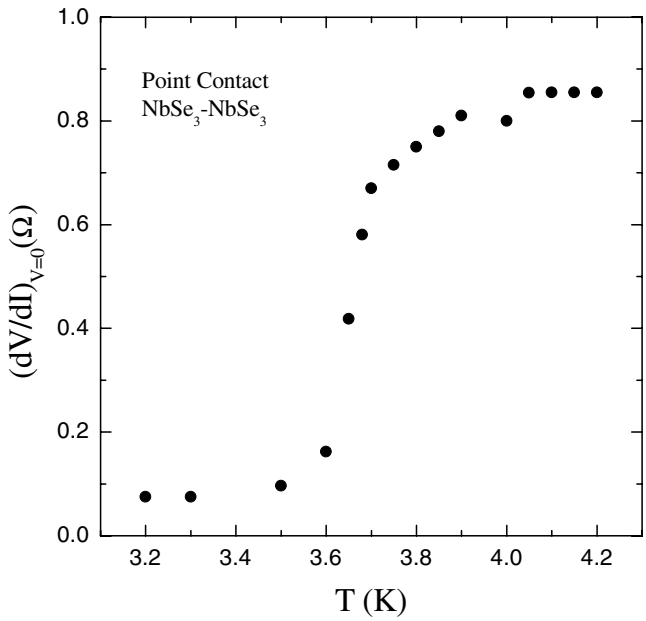

Figure 3. Differential resistance at zero bias $(dV/dI)_{V=0}$ against temperature for the junction of figure 1. Here we observe the evolution of the differential resistance at zero bias with temperature. The transition starts at about 4.15 K, and is completed at around 3.6 K. This is a clear indication that the feature observed in figure 1 is a transition to a superconducting state, and that we can associated it with a critical current.

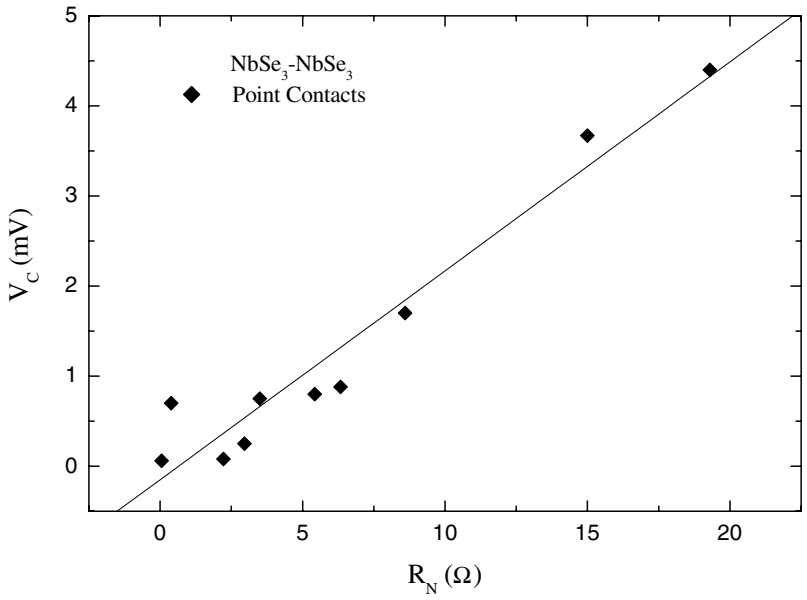

Figure 4. Critical voltage against normal resistance as measured for some of the junctions reported in this paper.

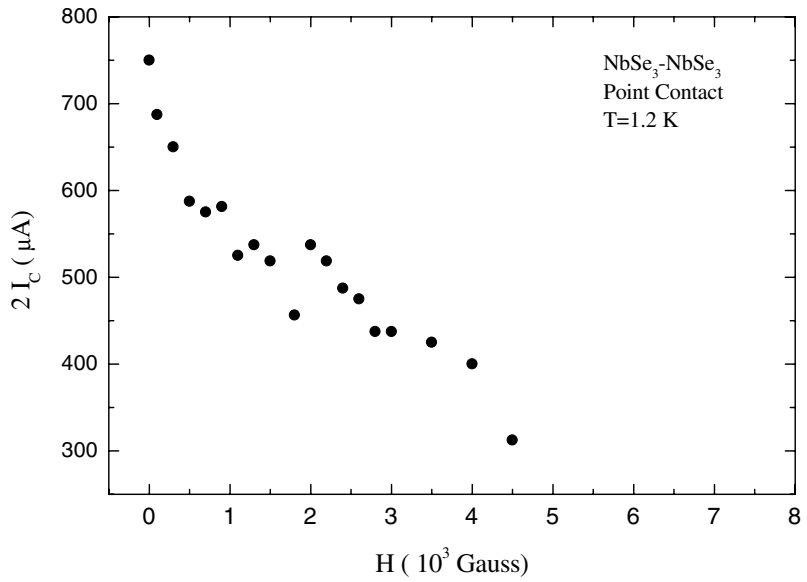

Figure 5. Evolution of the critical current as a function of the magnetic field applied perpendicular to the plane of the junction at a temperature of $T = 1.2$ K.

3. Analysis of the experimental data

The energy gap, $\Delta(0)$, and the strength of the electron–phonon coupling, $2\Delta(0)/k_BT_c$, may be calculated using the models of Kulik and Omel'yanchuk (KO) [10, 11] valid for short

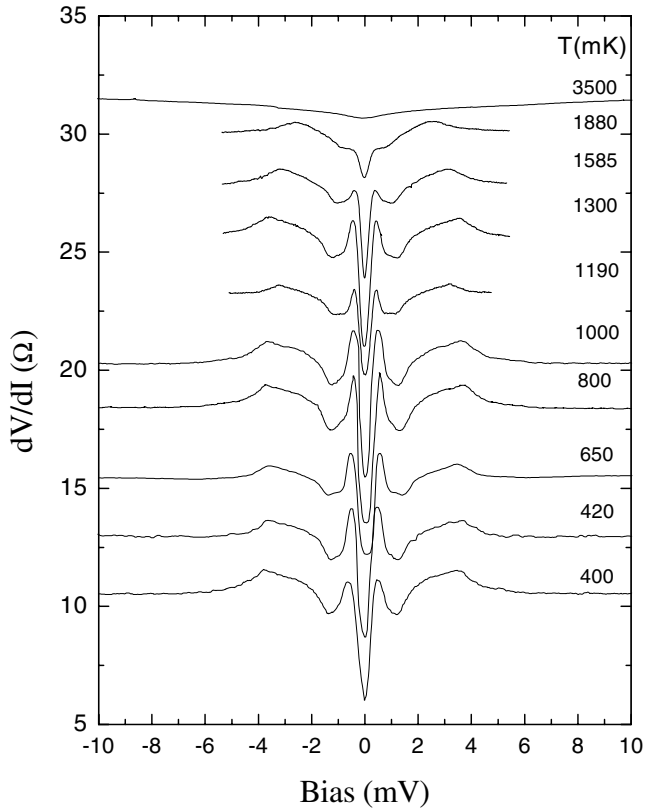

Figure 6. Differential resistance against bias voltage for a junction of $NbSe_3$–$NbSe_3$ from 0.400 K to 3.5 K, the curves are vertically displaced for clarity. The curve at 0.400 K is in the correct position with respect to the vertical scale in ohms. The horizontal scale was plotted only from −10 mV to +10 mV to show the finer details.

weak links in the dirty and clean limits, and the Ambegaokar and Baratoff (AB) model for superconducting tunnel junctions [12]. The zero temperature value of the critical current for these models, normalized to the $I_c(0)$ given by the AB model, is twice the AB value in the clean limit for short weak links [11], and is 1.32 times the AB value in the dirty limit [10]. The prediction of the AB model is plotted as a full curves in figure 2. At low temperatures the theoretical model fits the experimental data well, but deviates at high temperatures. This behaviour of the AB model is not surprising, because in most junctions it has been found to give only semiquantitative agreement. The critical current for this model is given by

$$I_c(T) = \frac{\pi \Delta(T)}{2eR_N} \tanh\left(\frac{\Delta(T)}{2k_B T}\right). \tag{2}$$

At zero temperature, the equation takes the form

$$I_c(0) = \frac{\pi \Delta(0)}{2eR_N} \tag{3}$$

where k_B and e have the usual meaning, R_N is the normal resistance of the contact. From here it is possible to use the experimental value of the critical current I_c, measured at the lowest temperature, to determine the energy gap. Although this model is appropriate for tunnel junctions, it has been used in the past for microcontacts with good results [13]. Comparing the

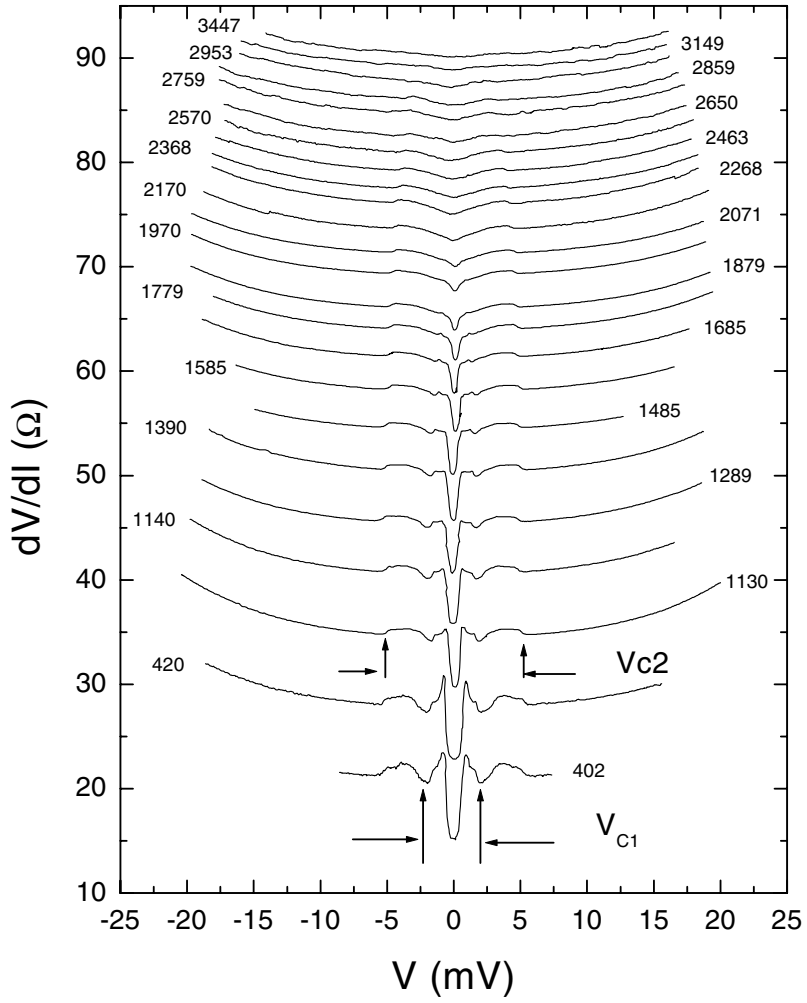

Figure 7. Differential resistance versus bias voltage for a junction of $NbSe_3$–$NbSe_3$ from 0.402 K to 3.44 K, the curves are vertically displaced. The curve at 0.402 K is in the correct position with respect to the vertical scale in ohms. Note that the horizontal scale is plotted from −25 mV to +25 mV (cf figure 6), to show the parabolic background. V_{c1} and V_{c2} are minima in the differential resistance that change with temperature.

shape of the critical current against temperature curves predicted by the KO and AB theories with the data of figure 2, it is clear they follow AB and the dirty limit of KO (cf figure 7.12c of [14][4]).

Using relevant parameters for this compound we can estimate the limiting values for the data. The electronic mean free path, l, for $NbSe_3$ is about 1000 Å, the superconducting coherence length ξ_0, determined using $\xi = 0.18\hbar v_F/k_B T_c \approx 460$ Å where the Fermi velocity was taken as $v_F = 1.4 \times 10^7$ cm s^{-1}, $T_c \simeq 4.2$ K, is $\xi_0 = \sqrt{\xi \times l} = 700$ Å. The conditions in the extreme dirty limit require that $l \ll \xi$ and $a > l$. Our junctions are in the limit $l \simeq \xi$

[4] There the behaviour of the temperature dependence of the critical current for tunnel junctions using the AB model and KO theories for short weak links in the clean and dirty limits is shown.

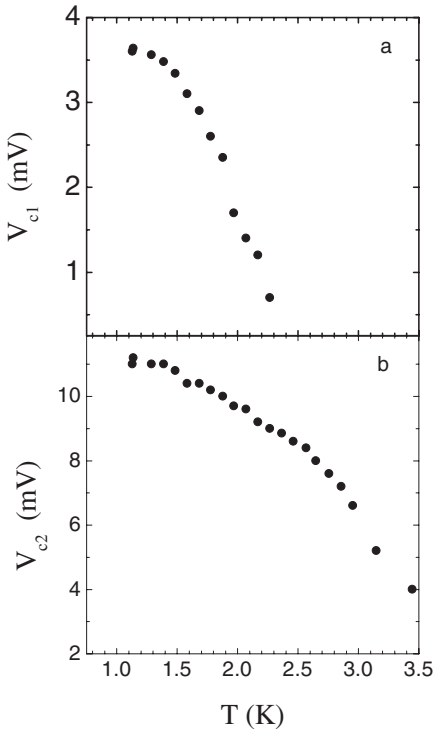

Figure 8. V_{c1} and V_{c2} are minima in the differential resistance shown in figure 7. We show the evolution with temperature of V_{c1} in (a) and the evolution of V_{c2} in (b).

and $a \simeq l$. Thus, our junctions are above the extreme dirty limit, and below the clean limit. The limiting values are between the ratio $1.32 < I_C(T)/I_C(0) < 2$. The limit for calculating the ratio must be close to 1.32. The ratio of the coupling strengths in the different limits are: 7.32 (AB), 5.3 (KO dirty limit) and 3.66 (KO clean limit). This analysis confirms that the ratio $2\Delta/k_BT_c = 7.32$, in the AB limit is very high. However the clean limit of KO is in the low limit. It is convenient to remember that the coupling strength for the CDW energy gap at $T_2 = 59$ K, measured by Fournel *et al* [15], using tunnelling spectroscopy, was high (about 14, see a discussion on this value in [15]) indicative of very strong electron–phonon coupling (apparently this is the trend in low-dimensional systems [16]). It should be noted that in order to observe features as that shown in figure 1, the resistance of the contact must be small $R_N \leqslant 20\ \Omega$. We define V_c as the voltage where the critical current is a maximum (see figure 1) and where the curve shows an inflexion point. A plot of V_c as a function of R_N (figure 4) shows that as the resistance of the contact decreases, the value of the I_c and the slope of the current against voltage increases. In figure 5 we show the critical current I_c as a function of magnetic field (H) for another junction, the maximum critical current is about 750 μA at 1.2 K. Figure 6, shows sets of typical $\mathrm{d}V/\mathrm{d}I$–V data from 0.400 K to 3.5 K for junctions of the form $NbSe_3$–$NbSe_3$; the curves have been displaced vertically to show more clearly the evolution with temperature; only the curve at 400 mK is at its real value of the differential resistance in ohms. The central peak is close to 6 Ω. The features observed are as follows.

(*a*) A central minimum peak in the differential resistance, related to the superconducting state. The peak diminishes and disappears at 2.2 K, which we take as the transition temperature.

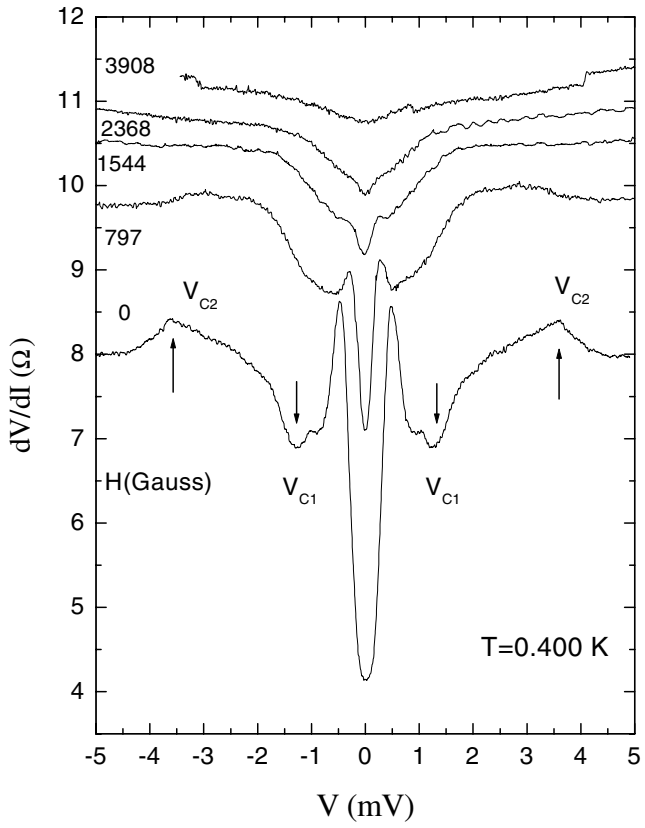

Figure 9. Differential resistance against bias voltage of a junction of $NbSe_3$–$NbSe_3$ at $T = 0.400$ K, as a function of the applied magnetic field in perpendicular direction to the plane of the junction.

(*b*) A broad maximum in differential resistance at around ±4 mV, which evolves slowly at low T and diminishes faster above 1.585 K; a faint anomaly can still be distinguished at 3.5 K.

Additional features can be seen in the data of another junction of $NbSe_3$–$NbSe_3$, shown in figure 7. Here the horizontal scale is from −25 mV to +25 mV. Again the vertical axis has been displaced, and only the data at 402 mK shows the real values of the differential resistance. The features are consistent with those on figure 6, except for a parabolic background. The central peak diminishes when the temperature is increased and disappears at about 2.650 K. A small symmetric minimum in the differential resistance with width of the order of 3.6 mV, which is marked by arrows and denoted in the plot as V_{c1}, persists, but diminishes as the temperature increases above 2.07 K. Another feature, marked by arrows and denoted as V_{c2}, diminishes as V_{c1} but more slowly at first, only to change rapidly at temperatures above 2.5 K and to fade away at about 3.4 K. Many other junctions showed the same symmetric features. The evolution of V_{c1} and V_{c2} shown in figures 8(a) and 8(b) represents the typical way the features evolve with temperature. V_{c1} disappears at around 2.3 K, and is related to the central peak; whereas V_{c2} persists above 3.5 K. Figures 9 and 10 show changes in $\mathrm{d}V/\mathrm{d}I$–V at two different temperatures as a function of a magnetic field applied perpendicular to the plane of the junction. The structure disappears as the magnetic field increases and the central peak (figure 9) disappears rapidly at small (1500 G) magnetic fields. The remaining structure disappears at higher fields (about 3900 G). The same trend is observed at other temperatures, but with a

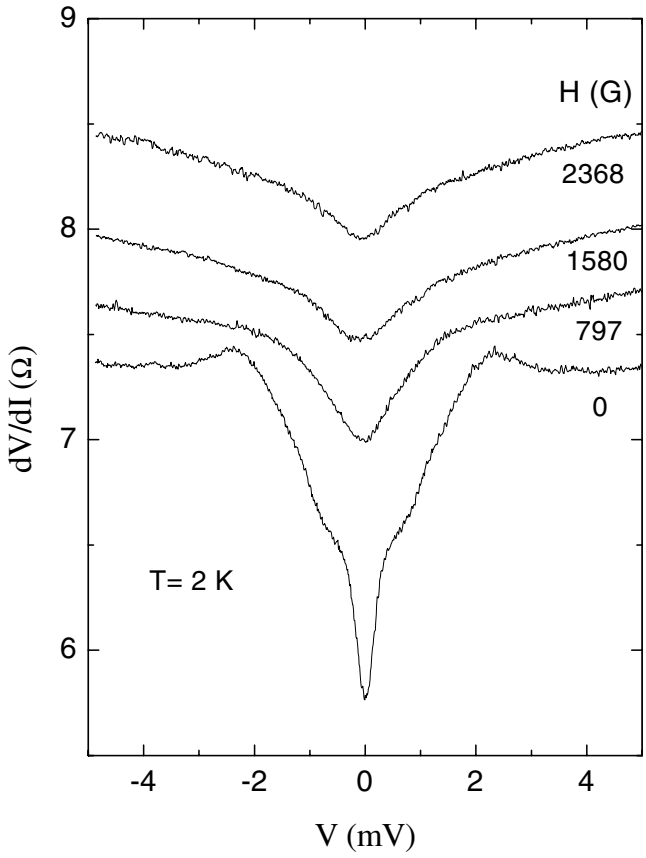

Figure 10. Differential resistance against bias voltage of a junction of $NbSe_3$–$NbSe_3$ at $T = 2.00$ K, as a function of the applied magnetic field perpendicular to the plane of the junction.

gradual decrease of the field needed to destroy the structure. V_{c2} may be associated with a second superconducting state in $NbSe_3$ with a higher T_c. This implies that the pressure is inhomogeneous. Normally, one would expect a range of superconducting states instead of the two states observed. It is possible that contact occurs at the edges of the $NbSe_3$ filament being used as the counter-electrode and that the pressures at each edge are different. Measurements on Au–$NbSe_3$ junctions (unpublished) show a similar effect. Experiments on different types of SN or SS constrictions show Andreev reflections in the dV/dI–V characteristics in the form of resistance peaks [17]. The voltage at which the peaks or dips are localized in the dV/dI curves show temperature dependences similar to the superconducting gap. As in the work of Westbrook and Javan[17], the preceding features occur at symmetric bias voltages which are well above the size of the energy gap (in our junctions about 1 mV using the ratio of the coupling strength that we determined ($7.32 \leqslant 2\Delta/k_BT_c \leqslant 5.3$), and in the range of the observed T_c. These features correspond to the destruction of superconductivity in small localized regions close to the contact area in which the current is injected. The current causes heating and creates a magnetic field. The magnetic vortices so created destroy the superconducting behaviour at small microscopic spots. This is a plausible explanation for the temperature dependence of the features, and also for the shape of the dV/dI curves with applied external magnetic field, as shown in figures 9 and 10.

4. Summary

We have performed extensive point contact experiments on $NbSe_3$ using a novel technique, and have shown that the pressure exerted by the counter-electrode ($NbSe_3$) makes the specimen ($NbSe_3$) locally superconducting. Hence, we have been able to study the superconducting behaviour of this low-dimensional system. We have found by comparing the critical current with the AB and KO theoretical models, the limit of the electron–phonon coupling is far above the BCS weak coupling limit. This result confirms that in superconducting low-dimensional systems, the electron–phonon interaction is very strong. In addition we found that above the superconducting transition a structure in the dV/dI against V characteristics is present. We associate this structure with those parts of the Fermi surface that remain nested after one or both CDWs have been almost destroyed by the local pressure created by the point contact. At this point it is important to remember that the superconducting behaviour at $T_c \approx 3.3$ K is accompanied by the destruction of the T_2 CDW, and whereas $T_c \approx 4.5$ K is due to the destruction of the T_1 CDW transition. Additional confirmation of this superconducting behaviour is found in the dependence of the critical current on the magnetic field. When an external magnetic field was applied to the junction, the critical current decreases in the same way as in a superconducting weak link.

Acknowledgments

This work was partially supported by grants of DGAPA-UNAM, and by the CONACyT-Mexico, through the bilateral program México–France and project G-0017.

References

[1] Monceau P (ed) 1985 *Electronic Properties of Inorganic Quasi-One-Dimensional Materials* vol II (Dordrecht: Reidel) pp 139–268
[2] Nuñez-Regueiro M, Mignot J-M and Castello D 1992 *Europhys. Lett.* **18** 53
Nuñez-Regueiro M, Mignot J M, Jaime M, Castello D and Monceau P 1993 *Synth. Met.* **55–57** 2653
[3] Ong N P and Monceau P 1977 *Phys. Rev.* B **16** 3443
[4] Briggs A, Monceau P, Nuñez-Regueiro M, Peyrard J, Ribault M and Richard J 1980 *J. Phys. C: Solid State Phys.* **13** 2117
Briggs A, Monceau P, Nuñez-Regueiro M, Ribault M and Richard J 1981 *J. Physique* **42** 1453
[5] Escudero R, Morales F and Lejay P 1994 *Phys. Rev.* B **49** 15 271
Escudero R, Lasjaunias J C, Calvayrac Y and Boudard M 1999 *J. Phys.: Condens. Matter* **11** 383
[6] Duif A M, Jansen A G M and Wyder P 1989 *J. Phys.: Condens. Matter* **1** 3157
[7] Wexler G 1966 *Proc. Phys. Soc.* **89** 927
[8] Yanson I K and Kulik I O 1978 *J. Physique* C **6** 1564
[9] Jansen A G *et al* 1980 *J. Phys. C: Solid State Phys.* **13** 6073
[10] Kulik I O and Omel'yanchuk A N 1975 *Zh. Eksp. Teor. Pis. Red.* **21** 216 (Engl. transl. 1975 *JETP Lett.* **21** 96)
[11] Kulik I O and Omel'yanchuk A N 1977 *Fiz. Nizk. Temp.* **3** 945 (Engl. transl. 1977 *Sov. J. Low Temp. Phys.* **3** 459)
[12] Ambegaokar V and Baratoff A 1963 *Phys. Rev. Lett.* **10** 486
Ambegaokar V and Baratoff A 1963 *Phys. Rev. Lett.* **11** 104
[13] Taguchi I and Yoshioka H 1970 *J. Phys. Soc. Japan* **29** 371
[14] See, for instance, Barone A and Paterno G 1982 *Physics and Applications of the Josephson Effect* (New York: Wiley) figure 7.12c, p 184
[15] Fournel A, Sorbier J P, Konczykowski M and Monceau P 1986 *Phys. Rev. Lett.* **57** 2199
[16] Hawley M E, Gray K E, Terris B D, Wang H H, Carlson K D and Williams J 1986 *Phys. Rev. Lett.* **57** 629
[17] Westbrook P S and Javan A 1999 *Phys. Rev.* B **59** 14 606